NASA TECHNICAL TRANSLATION

NASA TT F-422

NASA TT F-422
c. 1

A METHOD FOR THE NONDISPERSIVE ANALYSIS OF VERY LIGHT ELEMENTS

by Raymond Castaing and Françoise Pichoir

From *La Recherche Aérospatiale,*
No. 108, 1965

NATIONAL AERONAUTICS AND SPACE ADMINISTRATION • WASHINGTON, D. C. • JULY 1966

NASA TT F-422

A METHOD FOR THE NONDISPERSIVE ANALYSIS OF VERY LIGHT ELEMENTS

By Raymond Castaing and Françoise Pichoir

Translation of "Une méthode d'analyse non dispersive des éléments très légers."
La Recherche Aérospatiale,
No. 108, pp. 3-16, 1965

NATIONAL AERONAUTICS AND SPACE ADMINISTRATION

For sale by the Clearinghouse for Federal Scientific and Technical Information
Springfield, Virginia 22151 – Price $1.00

A METHOD FOR THE NONDISPERSIVE ANALYSIS OF VERY LIGHT ELEMENTS

Raymond Castaing and Françoise Pichoir

ABSTRACT

The adaptation to spectrographic analysis by X-ray emission of the double filter method initially suggested by Ross for diffusion studies has been extended to the analysis of the very light elements. For relatively low (2000 V) electron acceleration voltages, an important intensity of the characteristic X-radiation and a relatively high signal-to-noise ratio are obtained.

I. Introduction

The method of punctual analysis developed by one of the authors /3* (refs. 1, 2) and based on X-ray spectroscopy has had a wide range of applications in recent years. The possibilities of this method were also extended to the very light elements.

The elements with atomic numbers lower than 11 (sodium) are not easily analyzed by this technique: the sizable absorption of their characteristic lines and the absence of natural crystals with grating distances such that these crystals could be used as dispersive elements in the spectrograph make it difficult to analyze these elements by usual methods. As a result, during recent years, intensive research using microprobes was performed to determine the composition of the elements of the second line of the periodic table.

II. Various Methods Proposed

The first nondispersive method proceeds as follows: a global curve is determined by means of a proportional counter which receives the complex X-radiation emitted by the sample; this global curve is then broken up into its elements. Since we know the shape of the curve obtained by exciting pure samples we can find the concentrations of these pure elements with an electronic apparatus (ref. 3).

---

*Numbers given in margin indicate pagination in original foreign text.

A second method employs a spectrograph using a dispersive element having characteristics compatible with the wavelengths of the K-lines of the very light elements. The dispersive element is either an optical grating (refs. 4, 5) or an artificial crystal made up by the superposition of monomolecular layers of heavy stearates (barium stearate or lead stearate) (refs. 5, 6).

However, these dispersive methods can only be used for X-ray beams of small aperture, so that only a minute fraction of the radiation emitted by the sample can be analyzed.

Let us now consider the results obtained when using a differential filter method based on the principle put forward by Ross (ref. 7).

III. Principle

The intensity of any of the characteristic rays of the target element is very nearly proportional to its mass concentration. After one of the characteristic lines of an element is isolated from the background and from the other lines, it is possible to dose that element by comparing the intensities of the emitted target radiations to those emitted by a reference element of known composition.

However, the isolation of a given line can be achieved by a method of differential filtering based on the principle that, when subjected to X-ray radiations, each element possesses an absorption coefficient which varies very nearly as the cube of the wavelength (λ) exhibiting discontinuities for values of λ which correspond to the threshold excitation of the different energy levels of the atom. Therefore, for photons of wavelength λ, a filter composed of a given element exhibits a transmission factor equal to

$$\frac{I}{I_0} = \exp\left[-\mu(\lambda)\, x\right]$$

where x measures the thickness of the filter and μ denotes the linear absorption coefficient. /4

If we consider two filters composed of two neighboring elements in the periodic table, we can adjust the filter thicknesses so that they transmit equally the radiations with wavelength λ found outside the absorption discontinuities. For a given incident radiation, the difference in the intensities transmitted by the two filters measures the intensity of the fraction of the radiation carried by photons with a wavelength lying between the two discontinuities (fig. 1).

This method, called the Ross double-filter method, has been used by Cambou (ref. 8) for the dosage of zinc in the aluminum-zinc alloys with nickel and copper filters. The possibility of using this method in electronic probe microanalysis of relatively heavy elements was indicated as early as 1949 (ref. 9).

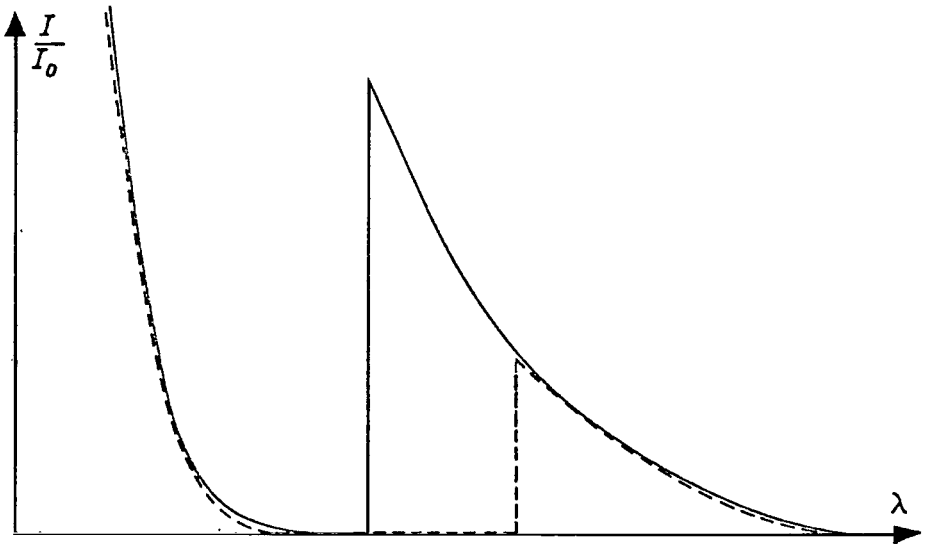

Figure 1. Variations of transmission factor of two neighboring elements in periodic table versus wavelength (thicknesses have been chosen so that both curves coincide as closely as possible outside the filter pass band).

——— Element with atomic number Z.
- - - - Element with atomic number Z-1.

The experiments described here deal mainly with the dosage of oxygen and nitrogen. We used gaseous filters, because the solid filters required for such an analysis involve numerous practical difficulties due to their minute thicknesses. For the dosage of oxygen the filters we used are composed, respectively, of oxygen and nitrogen in the gaseous form; for the dosage of nitrogen the filters were composed of nitrogen and methane. For the light elements, especially, the absorption jumps are different from one element to the next, which might introduce some difficulty. Section VII relates how this difficulty was overcome.

Such an analysis is a priori less precise than the analysis using a grating or a crystal as the dispersive element. The only dispersive element here is a proportional counter which cannot distinguish the K-lines from two neighboring elements. Furthermore, if the analyzed radiation contains L, M, or N...lines of heavier elements having wavelengths bounded by the two discontinuities of the filters (this band of wavelengths will be called the filter pass band), these radiations are found over the K-line of the analyzed element. On the other hand, this method enables us to analyze an X-ray beam of large aperture which is limited only by the size of the counter window. This large aperture allows us to deal with large transmitted intensities so that statistical fluctuations are reduced; relatively smaller accelerating voltages of the order of 2000 V can then be used. As a result, the depth of penetration of the electrons into the target is considerably reduced, which in turn means considerably smaller absorption corrections.

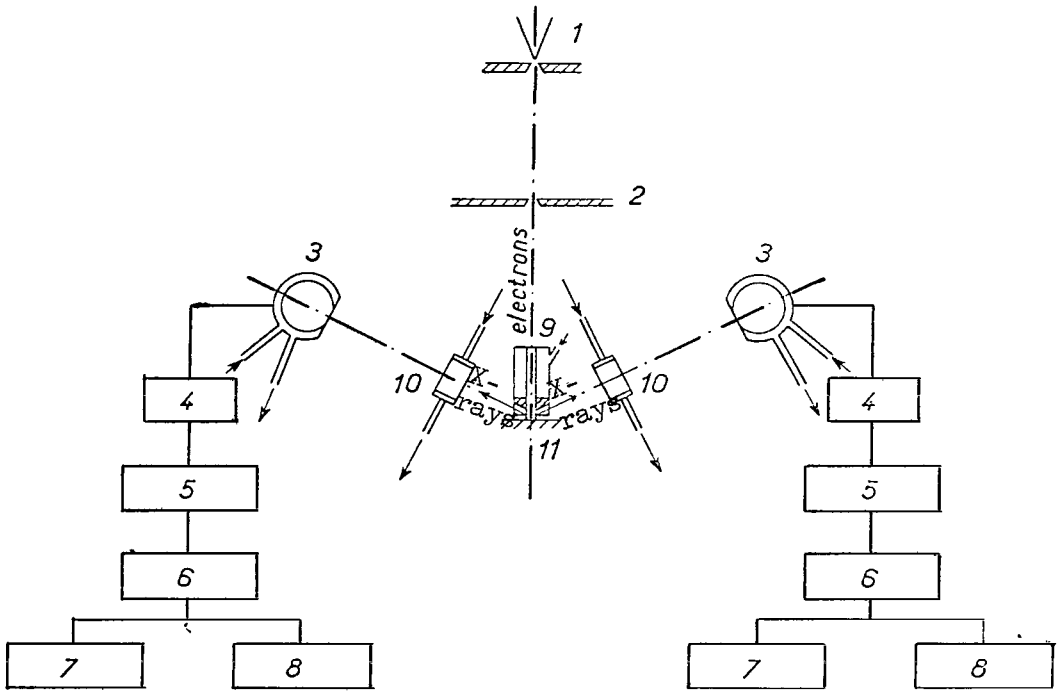

Figure 2. Diagram of experimental arrangement,

1. Electron gun
2. Diaphragm
3. Counters
4. Preamplifiers
5. Linear amplifiers
6. Amplitude selectors
7. Counting devices
8. Integrators
9. Cooling element
10. Filters
11. Sample

IV. Experimental Apparatus

The experimental apparatus (fig. 2) is composed of a 10^{-4} mm Hg vacuum chamber containing the electron gun, the anticontamination device, the sample to be analyzed, the reference samples, the filters, and the counters. Outside this chamber, two series of electronic devices count the number of impulses detected by the counters.

1. The RCA-type electron gun has a tungsten filament and can direct to the target sample an electron beam 1 mm in diameter. The voltage drop required to accelerate the electrons can be adjusted from 0 to 10 kV, but in most experiments is set at 2 kV with a current of 0.1 μA.

2. A hollow copper piece, cooled by liquid air, is an excellent anticontamination device. Apertures allow passage of X-rays and the electron beam. The cold walls located in the vicinity of the sample condense the organic vapors and thus considerably diminish the formation velocity of the contamination layer.

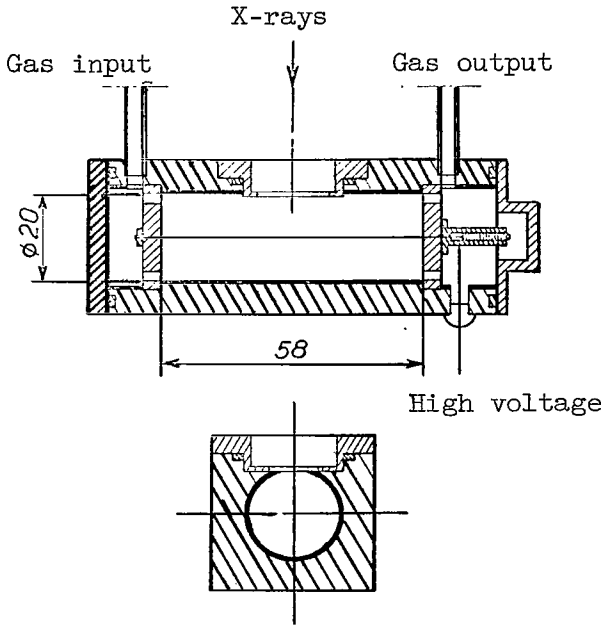

Figure 3. Diagram of counter.

3. The targets are mounted on a sample holder which supports the reference sample of known composition and the element used in the filter adjustment. /5

4. The filters are cylindrical containers closed at both ends by collodion windows. The pressure controlling the circulation of the absorbing gases can be adjusted. These gases enter and leave the filter through two tubes.

5. The proportional gas counters (argon and methane) (fig. 3) have an inside diameter of 20 mm. The input window is composed of a collodion film covered by a layer of aluminum 100 Å thick; this layer ensures the flowing away of the charges. The inside walls of the counter are also aluminum-covered. The fluorescence of this element is not bothersome since its K-line is sufficiently far from the lines of oxygen or nitrogen. The voltage drop can be adjusted from 0 to 2500 V and is applied to the central filament 25 μ in diameter. At atmospheric pressure the operating voltage is 2100 V.

6. The impulses from the counters are first amplified through a preamplifier with a gain of 30 (band width 500 kcps, noise level 125 μV), then through a linear amplifier. An amplitude selector and counting scales determine the number of impulses having an energy within V and V + ΔV. The displacement of the value V ranges from 5 to 40 V, with an adjustable range for ΔV varying between 0 and 5 V. Except when indicated, the value used for ΔV was 1 volt. With this arrangement we analyzed the distribution of the energy of the photons transmitted by the two filters. For each value of the energy we measured the difference in the transmitted intensities. The two series of electronic devices must have exactly the same gain, so that the two distributions of impulses furnished by the counters can be compared.

V. Preparation of the Windows Used In the Filters and In the Counters

These windows are composed of nickel grids with a mesh size of 250 μ /6 and a grid transparency of 64 percent. These grids are used as supports for two layers of collodion with an overall thickness of 1500 Å. The superposition of the two layers eliminates leaks due to occasional small holes in the film. This film is obtained by evaporation under vacuum of a solution of collodion plastified in butyl acetate.

VI. The Counters (10)

A certain number of the gaseous molecules are ionized by the passage of a photon with energy $h\nu$ as the latter enters the input window of a counter. The electrons so liberated are accelerated under the action of the radial field, and, after acquiring sufficient energy, cause a discharge in the neighborhood of the central wire. Each photon is then detected on the wire of the counter by an electrical impulse having an amplitude proportional to the energy of the incident photon. However, the linear characteristic of the response of the counters is subjected to limitations due to static fluctuations (ref. 11). A Gaussian distribution of the electrical impulses corresponds to a monoenergetic photon distribution. The width of the Gaussian curve measured at its midheight is at least equal to $0.354\ E^{1/2}$, where E is the photon energy expressed in /7 keV (fig. 4). This Gaussian curve can be sharpened by seeking optimal values of the inside diameter of the counter, the wire diameter, the gas pressure, and the nature of the gas. Due to instability of the amplification coefficient at low pressure, the counter must be operated at atmospheric pressure or higher. Furthermore, when we operate the counter at higher than atmospheric pressure, we eliminate all possibilities of leak of foreign gases into the counters, and the construction of the windows is simplified because they are subjected to a force always in the same direction. The axial wire on which the potential is applied must not be too thin, because irregularities in its diameter are responsible for the flattening of the Gaussian curve. When these two elements are imposed, the inside diameter of the counter is practically determined. An appreciable improvement in the sharpness of the crest of the Gaussian curve is obtained by using a gaseous mixture rich in methane (argon 35 percent, methane 65 percent) instead of the mixture commonly used until now (argon 90 percent, methane 10 percent).

VII. Filter Adjustments

We must first point out that the mechanism for the attenuation of an X-ray beam does not reside solely in photoelectric absorption. For wavelengths of 10-100 Å the classical diffusion of photons which is nearly independent of the wavelength is superposed on the photoelectric effect. As a result, it introduces an error, because this diffusion effect is different in two filters. This effect can be neglected.

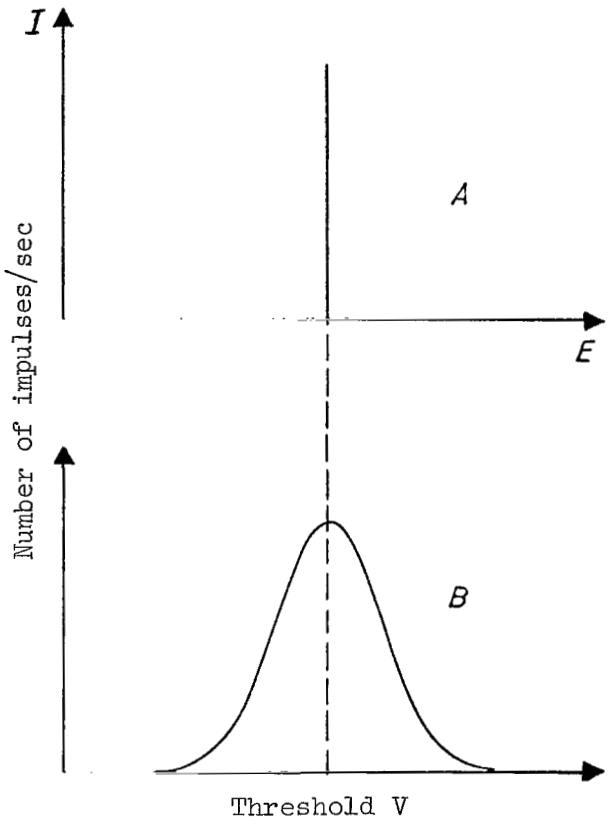

Figure 4. Response curve of proportional gas counter when impinged by monoenergetic photon flux: A, photon energy distribution; B, impulse energy distribution.

For filter adjustment, the absorption curves of the two filters must coincide outside the pass band of the filter. But the absorption jump varies from one element to the other and these two curves cannot be superposed exactly (fig. 5). However, if we add to element B an element C which does not exhibit any absorption jumps in the vicinity of the wavelengths under consideration, the absorption jump of the mixture B + C will be decreased. The mass absorption coefficient of the mixture is equal to

$$\frac{\mu_{BC}}{\rho_{BC}} = \frac{\mu_B}{\rho_B}\alpha_B + \frac{\mu_C}{\rho_C}\alpha_C$$

where α_B, α_C represent, respectively, the percentages of the masses of B and C in the mixture B + C. By properly choosing C and the proportions α_B and α_C, we can make the two curves coincide.

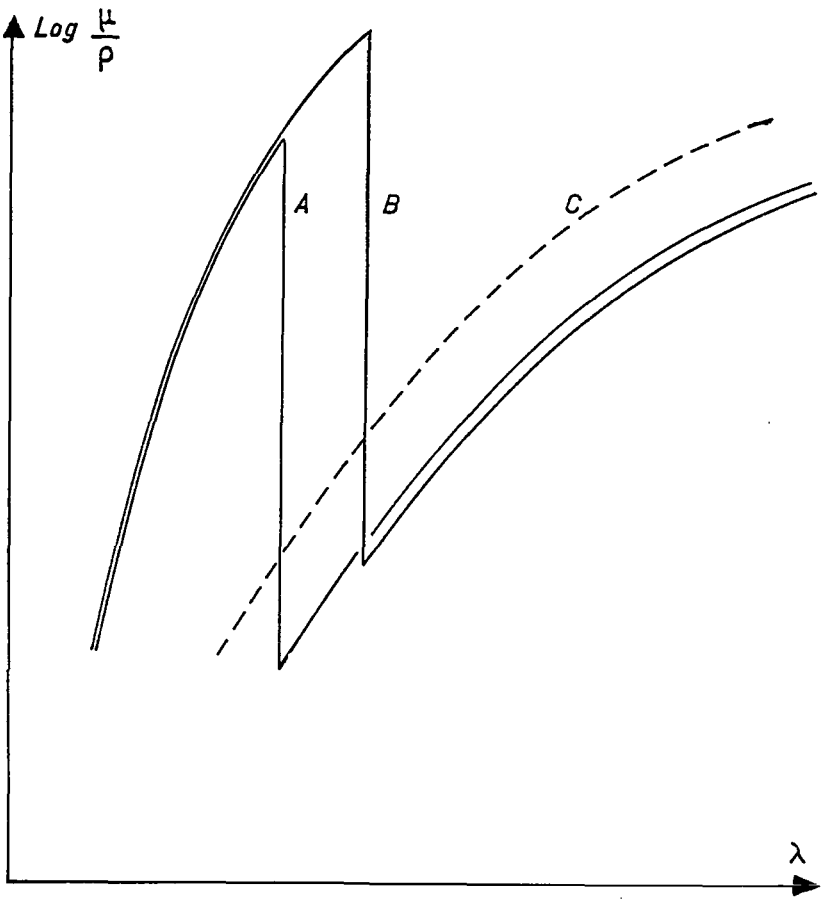

Figure 5. Variations of absorption coefficient for two adjacent elements A and B and of auxiliary element C in terms of wavelength.

For the dosage of oxygen, the additive element chosen was krypton, which has L discontinuities in the vicinity of 8 Å. A gaseous mixture, under suitable pressure and containing 99.4 percent nitrogen and 0.6 percent krypton, has the same absorption curve as oxygen in the two spectral regions for values of the wavelength outside the filter pass band. For the nitrogen dosage, the methane and nitrogen filters are adjusted without addition of a third element. The hydrogen present in the methane acts as the third element.

We must carefully select the filter and counter windows, so that the global absorption through the collodion film becomes identical on each of the two paths. For elements such as nitrogen or boron these absorptions are not small. The three windows have a total thickness of 4500 Å of collodion, and the transmission factor for the characteristic K-line of boron is only 40 percent. The counter windows are then covered with an aluminum layer in pairs by evaporation under vacuum, so that each pair receives the same thickness of metal. The control measurements are made directly on the experimental setup. We measured the

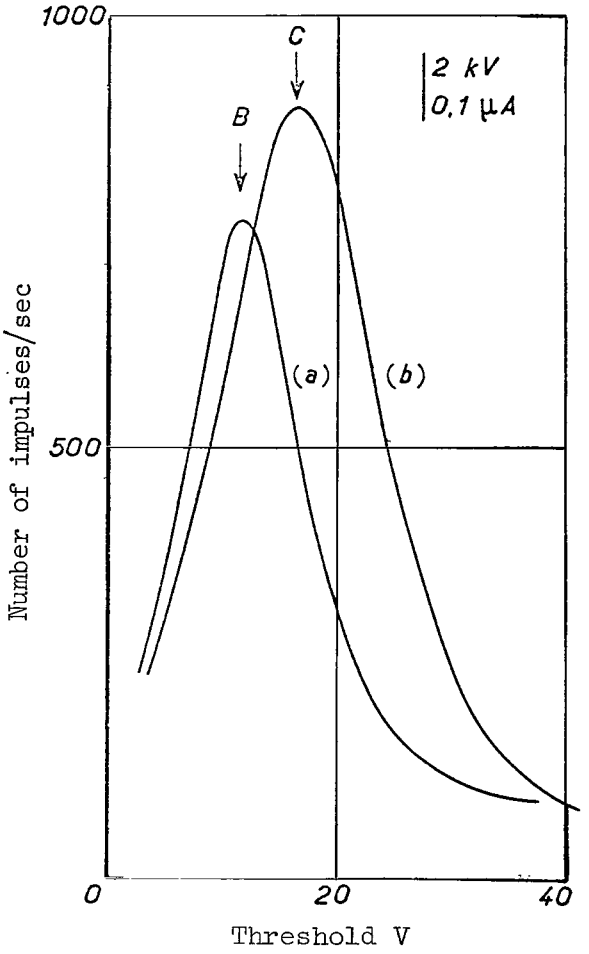

Figure 6. Experimental curves of nonfiltered radiation: (a) boron sample; (b) carbon sample.

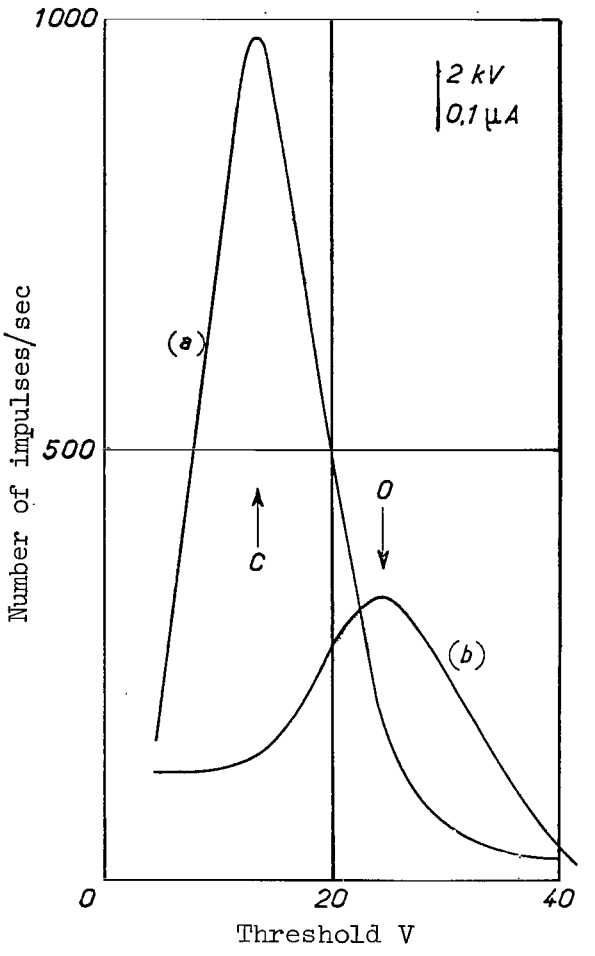

Figure 7. Experimental curves for nonfiltered radiations: (a) carbon sample; (b) beryllium oxide.

K-line of boron simultaneously on both paths, the two filters not containing any gas. Once this adjustment is made, gases are introduced in the filters and the pressure is adjusted so that the radiation of a reference element, having a characteristic line outside the filter pass band, is identically absorbed on both paths.

In the case of the analysis of oxygen, the reference element is a sample of boron nitride; in the case of nitrogen, we used the K-radiation of carbon.

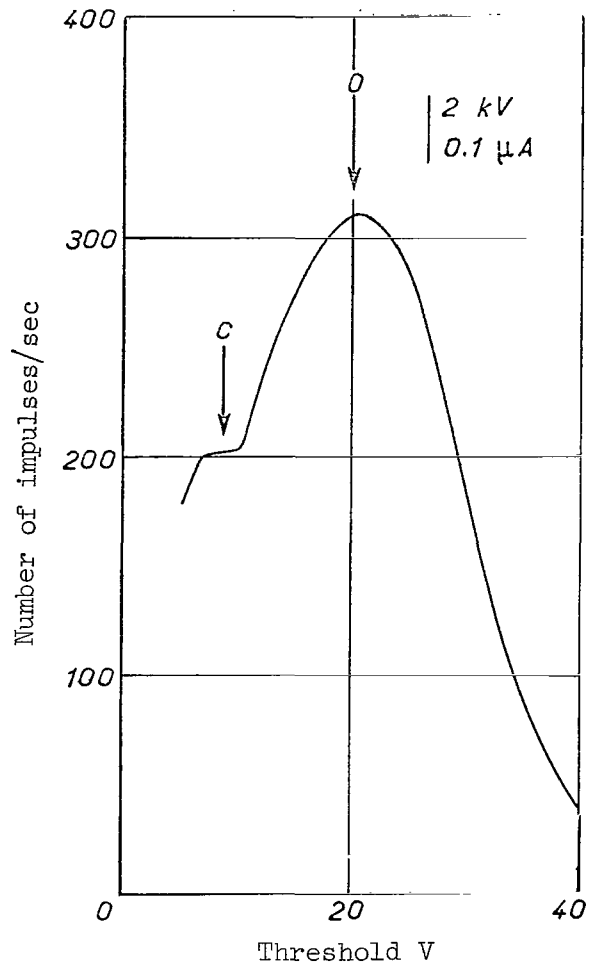

Figure 8. Experimental curve for nonfiltered radiation of lithium carbonate.

VIII. Results

All the depicted curves have the applied threshold voltage in the abscissa and the number of impulses per second in a range of 1 volt in the ordinate. The applied threshold voltages are proportional to the photon energies and to their frequencies. The curves were obtained point by point in 2-volt intervals.

VIII. 1. Direct radiations

Curves 6, 7 and 8 represent the nonfiltered radiation of anticathodes /8 of boron, carbon, beryllium oxide and lithium carbonate. In the particular case of the lithium carbonate, the two curves of carbon and oxygen are not

distinguished by the counter. It is necessary to filter the global radiation in order to isolate the oxygen. For example, in figure 17 the curve obtained, after using the oxygen filter, would be carbon. We checked on the curves the proportionalities of the threshold voltages to the energies of the X photons. The wavelengths for the K-line of boron, carbon and oxygen are, respectively, equal to 67.6, 44.7 and 23.32 Å.

VIII. 2. Filtered radiations

General aspect of the curves

For each sample we plotted three distinct curves. The highest corresponds to the intensity transmitted in the pass band by the less absorbant filter, the lowest corresponds to the other filter (these two curves are shown as dotted curves); the third curve is obtained by subtracting the second curve from the first. This last curve, shown as a full curve, represents the contribution of the analyzed element to the overall radiation. We call such a curve a differential curve.

If the transmission factor of the two filters are identical outside the filter pass band, the two curves representing the transmitted intensities must coincide at their two end points. However, such a coincidence does not take place when the threshold potential reaches values corresponding to the energies of the discontinuities. This coincidence takes place in a progressive manner on both sides of the filter pass band when we move away from such a range of wavelengths, because the counter "spreads" the X-radiation transmitted by the filters. This point will be discussed later.

The dosages are made by setting the band ΔV at the maximum of the "differential curve." The unknown sample and the reference sample of known concentration are brought successively under the impact of the electron beam, and we note in each case the difference in the values obtained on the two paths. This difference is very nearly proportional to the mass concentration of the /9 element considered in the sample.

The measurements can be made in a 1 V step, as is the case for the measurements that follow, or on the entire curve. The number of impulses in the latter case is multiplied by a factor of approximately 10.

Oxygen dosage

The dosages were made on samples of lead oxides PbO and PbO_2, on copper oxides Cu_2O and CuO, and on Fe_3O_4 and CO_3Ca. Our reference sample was lithium carbonate CO_3Li_2 (figs. 11 to 17). Figure 9 shows variations of the transmission factor of the oxygen and nitrogen filters in terms of the wavelength. The wavelengths of the K-lines of the elements written above the curves enable us to read directly the transmission factors of the filters for each radiation.

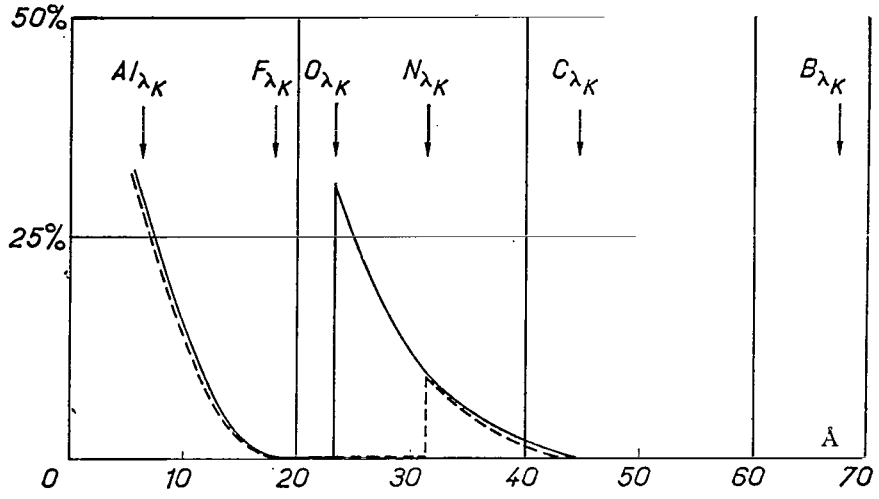

Figure 9. Variations of transmission factor in terms of wavelength.

——— Transmission factor for oxygen filter.
– – – – Transmission factor for nitrogen-krypton filter.

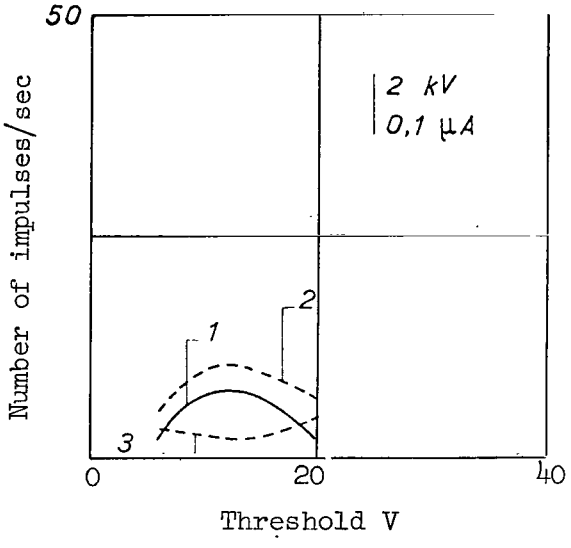

Figure 10. Evaluation of continuous background. Gold sample. 1, Differential curve; 2, oxygen filter; 3, nitrogen filter.

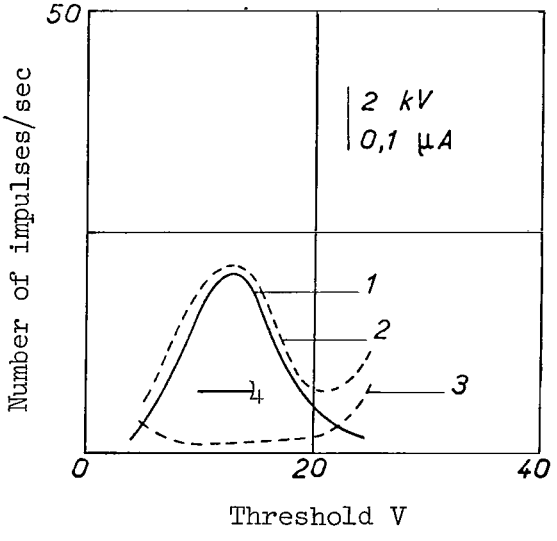

Figure 11. Dosage of oxygen in lead monoxide PbO. 1, Differential curve; 2, oxygen filter; 3, nitrogen filter; 4, background.

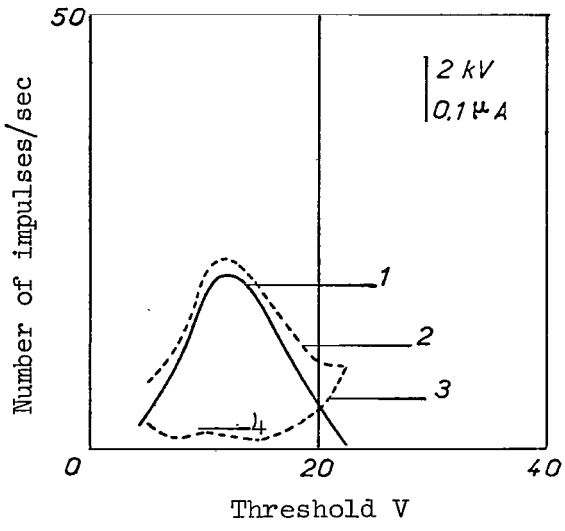

Figure 12. Dosage of oxygen in copper oxide Cu_2O. 1, Differential curve; 2, oxygen filter; 3, nitrogen filter; 4, background.

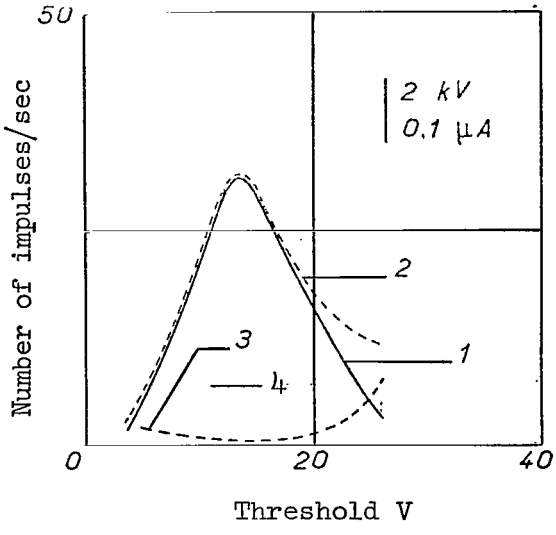

Figure 13. Dosage of oxygen in lead dioxide PbO_2. 1, Differential curve; 2, oxygen filter; 3, nitrogen filter; 4, background.

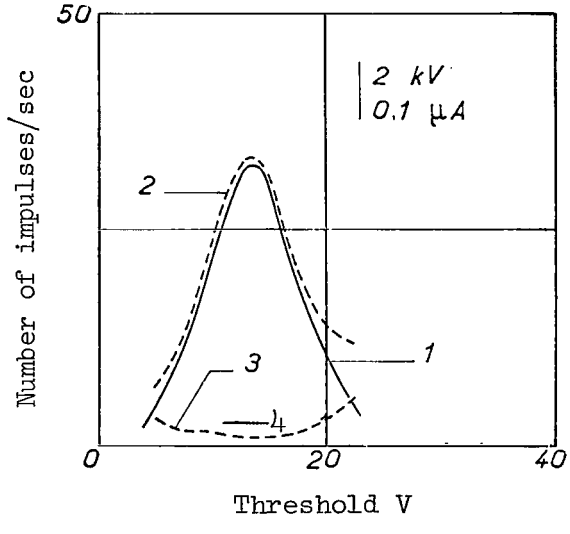

Figure 14. Dosage of oxygen in copper oxide CuO. 1, Differential curve; 2, oxygen filter; 3, nitrogen filter; 4, background.

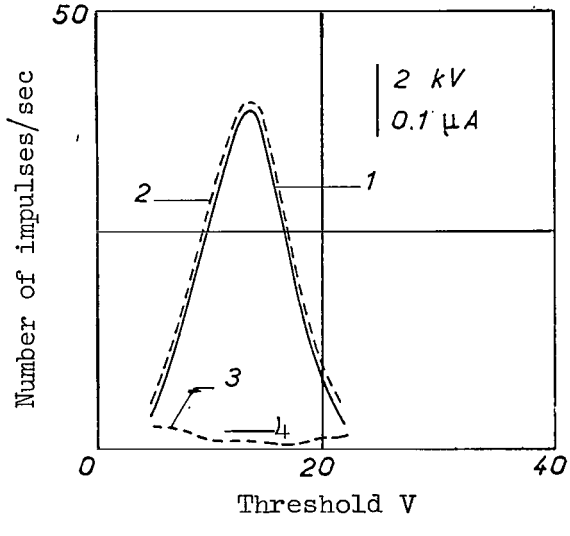

Figure 15. Dosage of oxygen in magnetic iron oxide Fe_3O_4. 1, Differential curve; 2, oxygen filter; 3, nitrogen filter; 4, background.

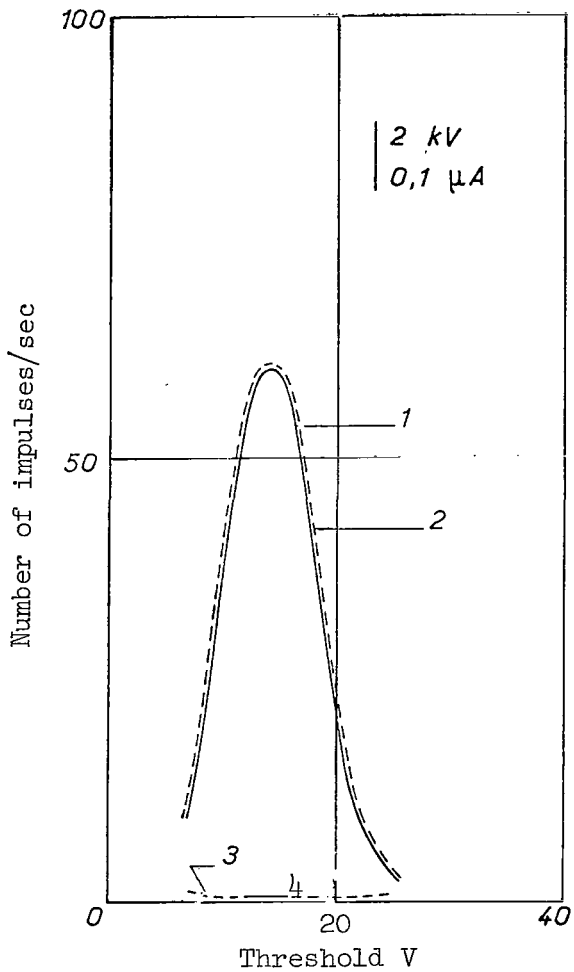

Figure 16. Dosage of oxygen in calcium carbonate CO_3Ca. 1, Differential curve; 2, oxygen filter; 3, nitrogen filter; 4, background.

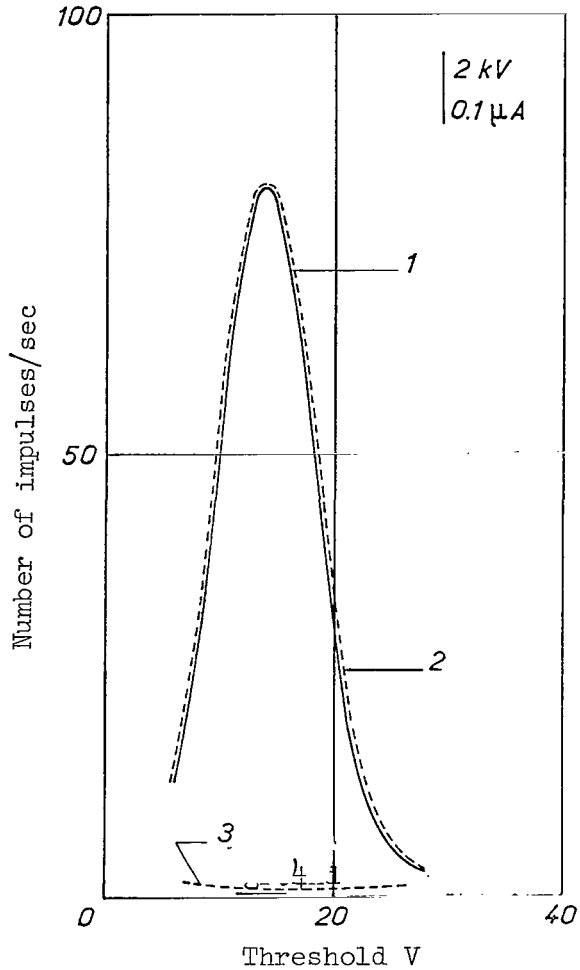

Figure 17. Dosage of oxygen in lithium carbonate CO_3Li_2. 1, Differential curve; 2, oxygen filter; 3, nitrogen filter; 4, background.

Most of the plotted curves exhibit an increase near the short wavelengths (figs. 11 to 14). For these wavelengths the transmission factor of the filters increases monotonically as λ decreases. In the case of lead oxides the background is transmitted more and more; for copper oxides, in which the background is less important, the curves representing the transmitted intensity /11 suffer an increment due to the presence of the L-line of copper at 13.3 Å.

Figure 18 displays good proportionality between emission and concentration. Table 1 exhibits the intensities measured at the maximum of the differential curves. Figure 18 shows these intensities corrected for background and expressed in percentage with respect to pure oxygen. I_0, the emission intensity for pure oxygen, was computed from mesasurments made on the lithium carbonate reference sample.

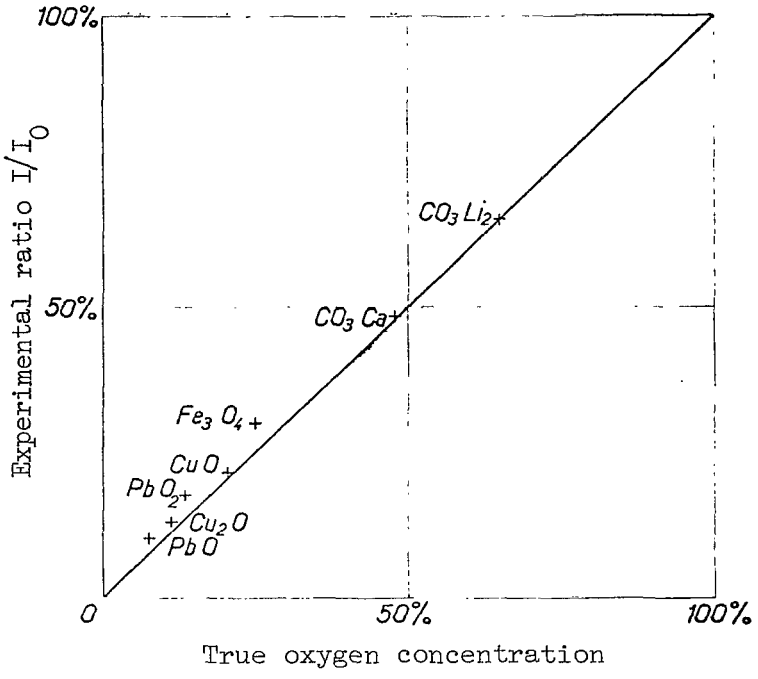

Figure 18. Oxygen dosage in various samples.

TABLE I. OXYGEN DOSAGE

	Average atomic number $\bar{Z}$	Total intensity I (impulses/sec)	Background (impulses/sec)	Intensity corrected for background (impulses/sec)	Experimental ratio I/I_0	True oxygen concentration
Au	79	7.8	7.8	0	0	0
PbO	76.6	19.8	7.6	12.2	0.10	0.072
Cu_2O	26.5	18.3	2.7	15.6	0.128	0.112
PbO_2	72.1	28.4	7.2	20.8	0.17	0.134
CuO	24.8	28.3	2.4	25.9	0.212	0.20
Fe_3O_4	21.1	39.5	2.1	37.4	0.306	0.276
CO_3Ca	11.8	60	1.2	58.8	0.481	0.48
CO_3Li_2	6.73	80	0.6	79.4	0.65	0.65

Influence of the continuous spectrum

The filters transmit the characteristic lines and the background between /12
the two discontinuities. When the sample is composed of heavy elements, the background becomes important. Determination of the intensity of this background in the case of gold, having atomic number Z = 79 (fig. 10), enables us to estimate its intensity for the other samples. We have assumed that the intensity of the continuous spectrum is proportional to the average atomic number $\bar{Z}$ of the sample, where $\bar{Z}$ is defined for the compound AB having C_{mA} and C_{mB} as the mass concentration of elements A and B by the relation

$$\bar{Z}_{AB} = C_{mA}Z_A + C_{mB}Z_B.$$

We know, empirically, that a similar relation holds true when more than two elements are found in a given sample.

Nitrogen dosage

Figure 19 represents the variation of the transmission factor of the /13
nitrogen and methane filters as compared to the wavelength. The dosages were made on samples of boron nitride, chromium nitride and silicon nitride; as an example, the curves relative to the boron nitride are shown in figure 20. We also analyzed a sample obtained by mixing copper powder with silicon nitride powder, the last element having a nitrogen concentration of 4 percent by weight. In the filter pass band, the ratio of the intensities emitted, respectively, by the sample and by a pure copper reference sample was found to be 2:4. We deduced that the intensity of the line emitted by pure nitrogen in the same pass band would be $1.4/0.04 = 35$ times greater than the fraction of the continuous spectrum emitted under the same conditions by the pure copper sample. By assuming that the background intensity is nearly proportional to the average atomic number, we find that in the case of a sample of pure nitrogen and for an accelerating voltage of 2000 V the ratio of signal to background noise is

$$\frac{35 \times 29}{7} = 145.$$

Let us point out that such a signal-to-noise ratio permits an easy dosage of nitrogen in samples of average atomic number close to that of copper and containing a nitrogen concentration of the order of 1 percent.

Table II displays results of the nitrogen analyses.

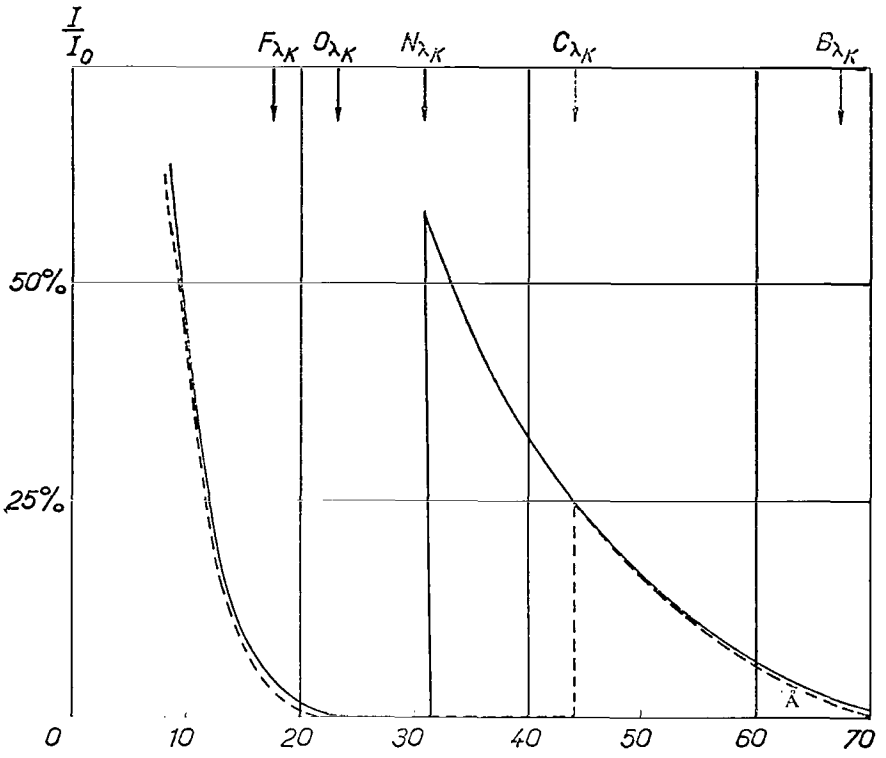

Figure 19. Variation of transmission factor in terms of wavelength.

——— Transmission factor for nitrogen filter.
---- Transmission factor for methane filter.

IX. Discussion of Results

IX. 1. Experimental determination of the intensity of the background found in the filter pass band

Let us consider the curve giving the number of impulses per second in terms of the threshold voltage of the amplitude selector. These impulses per second are registered by the counter, with no filter, and the sample is a pure element, such as carbon. If the sample did not emit a continuous spectrum and if the range of amplitudes allowed by the amplitude selector were infinitely narrow, this curve would represent the amplitude distribution of the impulses given by the counter for a single line, in this case, the K-line of carbon. Such a curve would resemble a Gaussian curve. Its width at midheight is imposed by the statistical fluctuations of the number of primary ionizations generated in the counter gas by the K photons of carbon. We will assume that such a curve would remain nearly Gaussian (its width at its midheight being slightly increased) for a small but nonzero value of the range of amplitudes admitted by the selector (1 V, for example).

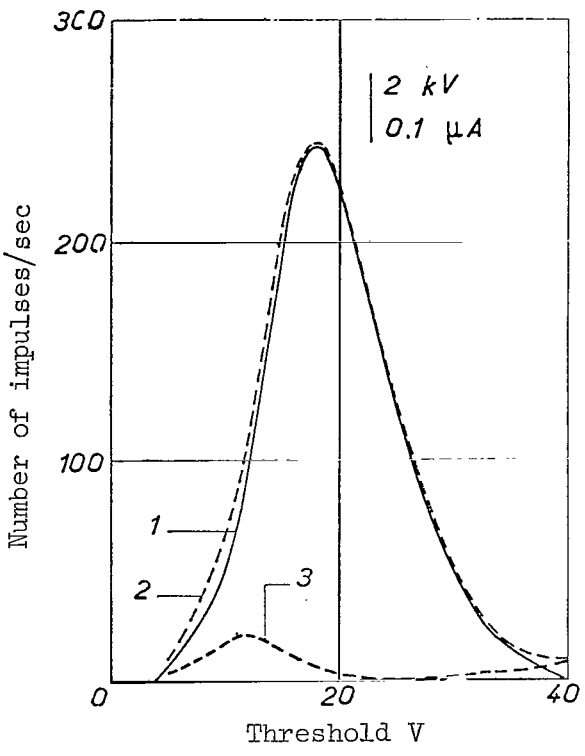

Figure 20. Nitrogen dosage in boron nitride BN. 1, Differential curve; 2, nitrogen filter; 3, methane filter

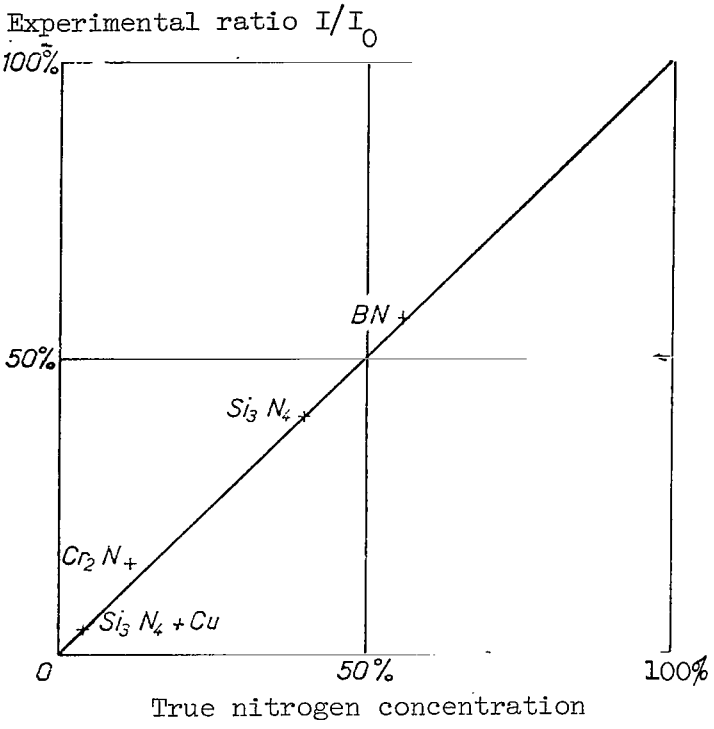

Figure 21. Nitrogen dosage in various compounds.

TABLE II. NITROGEN DOSAGE.

	Average atomic number $\bar{Z}$	Total intensity I (impulses/sec)	Background (impulses/sec)	Intensity corrected for background	Experimental ratio I/I_0	True nitrogen concentration
Au	79	34.3	34.3	0	0	0
Si_3N_4 + Cu	27.2	29.8	11.8	18	0.042	0.04
Cr_2N	22	72.8	9.5	63.3	0.148	0.119
Si_3N_4	11.2	173.1	4.9	168.2	0.396	0.40
BN	6.1	242.6	2.6	240	0.564	0.564

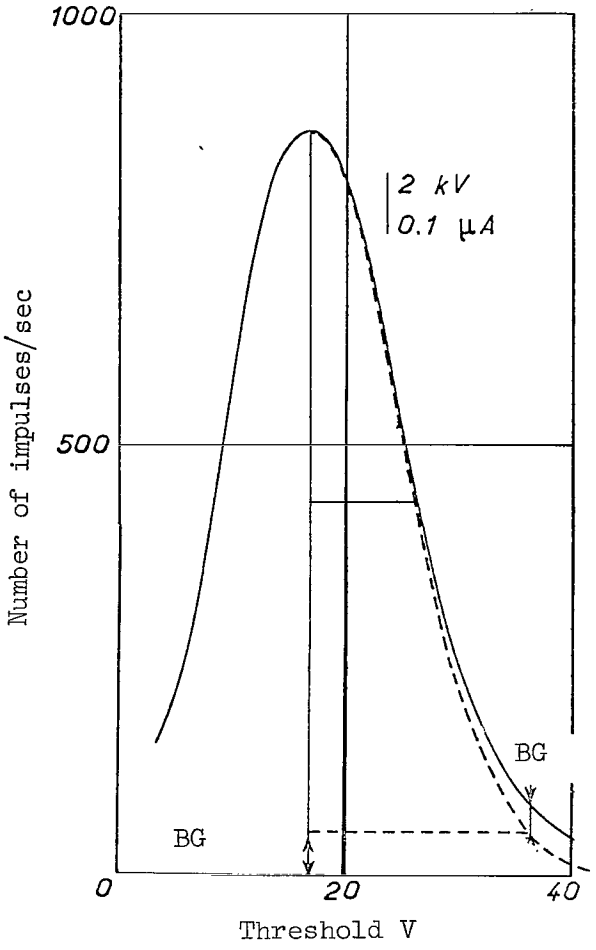

Figure 22. Evaluation of spectrum using nonfiltered radiation of carbon; BG, background.

——Experimental curve.
----Theoretical curve for the pure K-line.

The actual curve, as measured on the carbon sample (fig. 22), differs from the Gaussian curve by the presence of "tails" due to the continuous spectrum. These tails extend this curve on both sides (small and large threshold values) without appreciably modifying the shape of the curve's central portion.

We can therefore estimate the importance of the continuous spectrum by plotting on the diagram a Gaussian curve matching the experimental curve on the entire central portion. This curve is then extrapolated on the large threshold voltage values. The difference in the ordinates between the experimental and the Gaussian curves (taken for an abscissa not too distant from the central region) gives a rough estimate of the importance of the continuous spectrum at the level of the

carbon line. Experiments show that this difference of ordinates remains /14
nearly constant when the threshold voltage varies from 5 to 10 V. Such a result agrees well with the fact that the intensity of the continuous spectrum is a slowly varying function of the wavelength in the region distant from the quantum limit corresponding to an energy of 2000 eV. Furthermore, the spreading due to the statistical fluctuations of amplitude further decreases that intensity variation. A relatively wide band of the continuous spectrum contributes to the production of impulses of a given height.

By using this method, we find experimentally that in the case of carbon the contribution of the continuous spectrum at the level of the characteristic line is of the order of 1/20 of the intensity of that line.

In the case of a differential analysis the signal-to-noise ratio is considerably improved: on one hand, the portion of the continuous spectrum corresponding to wavelengths outside the pass band, after crossing the filters, yields equal intensities that cancel out after we take the differences of these measurements. On the other hand, the pass band is narrower than the band of sensitivity of the counter. Furthermore, inside the pass band the transmission factor of the carbon filter--very large for the carbon K-line which lies very close to the lower discontinuity in the wavelength scale--decreases rapidly when the wavelength increases. As a result, the average transmission factor for the portion of the continuous spectrum lying inside the pass band is weaker than the transmission factor for the characteristic line of carbon. The ratio of these two transmission factors decreases as the filter thickness increases. This can be used to improve the signal-to-noise ratio. However, we cannot proceed far in this direction, because this improvement is made at the expense of the intensity of the transmitted characteristic line and therefore at the expense of the sensitivity of the measurements.

We can measure experimentally by two different methods the importance of the contribution of the continuous spectrum when differential-filter analysis is used.

(a) We measure the difference of the transmitted intensities in the case of a sample composed of a pure element with atomic number Z. This sample is selected because its characteristic line is not found in the filter pass band. Let I_Z be the value so obtained. Assuming that the intensity of the continuous spectrum (c.s.) is proportional to the atomic number, for an analyzed element of atomic number $\bar{Z}$ we can write the intensity of the portion of the continuous spectrum which adds up to the characteristic line as

$$I_{c.s.} = I_Z \frac{\bar{Z}}{Z} .$$

(b) For an anticathode we can use an auxiliary compound having the same average atomic number as the sample but with its characteristic line outside the filter pass band. We can then directly measure the difference in the transmitted intensities by the two filters.

IX. 2. Absorption corrections

There is a lack of information on values of the absorption coefficients in that range of wavelength and nothing has been written about the distribution in depth of the characteristic emission for such small accelerating voltages. However, let us point out that for our experimental conditions the absorption corrections are quite small, at least in the case of pure elements. Let us consider as an example a carbon target bombarded by 2000 eV electrons. The thickness (measured in mass per unit surface area) of the superficial area, which emits the K-characteristic radiation, is less than 0.02 mg/cm^2. Thus, if the mass absorption coefficient is equal to 2000 and the angle of emergence is 30^o, the average absorption is of the order of 4 percent. However, if the accelerating voltage of the beam is of the order of twenty kV, the depth of average emission reaches 0.5 mg/cm^2 and the absorption in the sample becomes 80 percent. This absorption would be even higher in the case of the analysis of carbon embedded in a matrix of a heavy element, and the measurements would lose practically all their significance. It is therefore essential that the electron accelerating voltage be small. An anticontamination system is then indispensable.

IX. 3. Lines L, M, N,... of heavy elements

Lines L, M,... that fall within the filter pass band will add to the /15
K-line intensity of the element under consideration. It is possible to evaluate the importance of these spurious lines by measuring their emission on the pure elements. If we know the proportion of the heavy element in the compound, we can calculate the intensity of the L, M,... lines provided that intensity of these lines is proportional to the concentration of the corresponding elements.

Table III lists the elements having some of their characteristic lines in the pass bands corresponding to the oxygen and nitrogen filters.

According to our measurements, a pure titanium sample emits in the /16
pass band, corresponding to the dosage of oxygen, an intensity (L-line) which represents about 25 percent of the intensity of the K-line emitted under the same conditions by a pure oxygen sample. On the other hand, lead and niobium have no visible contribution at the nitrogen level.

TABLE III

Lines	Oxygen	Nitrogen
L	Titanium - Vanadium - Chromium	Calcium - Scandium - Titanium
M	Ruthenium - Rhodium - Palladium Cadmium - Tin - Antimony - Tellurium	Niobium - Molybdenum - Ruthenium - Rhodium Palladium - Silver - Cadmium - Tin
N		Lead - Thorium - Uranium

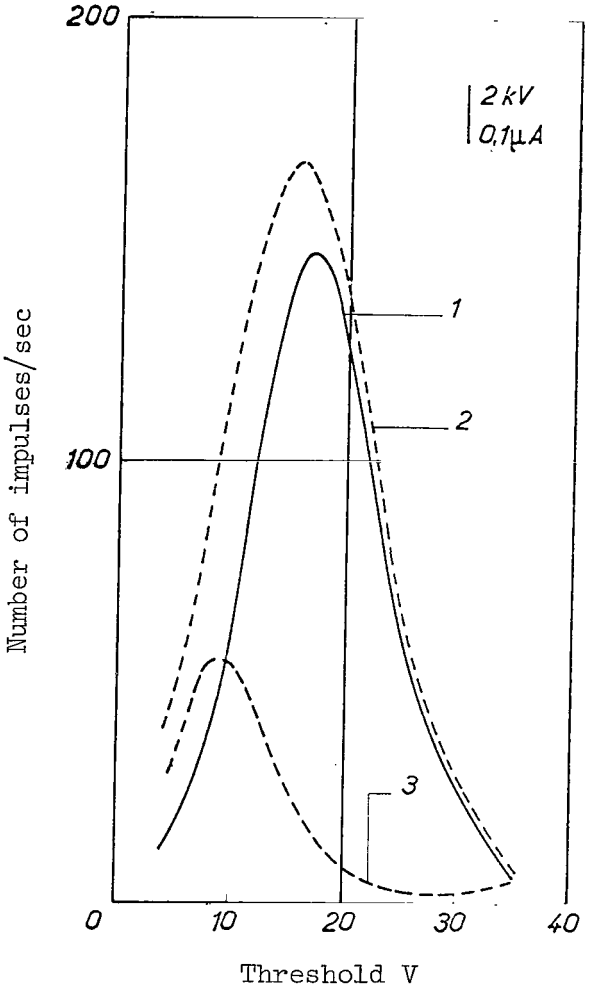

Figure 23. Nitrogen dosage in boron nitride without anticontamination device. 1, Differential curve; 2, nitrogen filter; 3, methane filter.

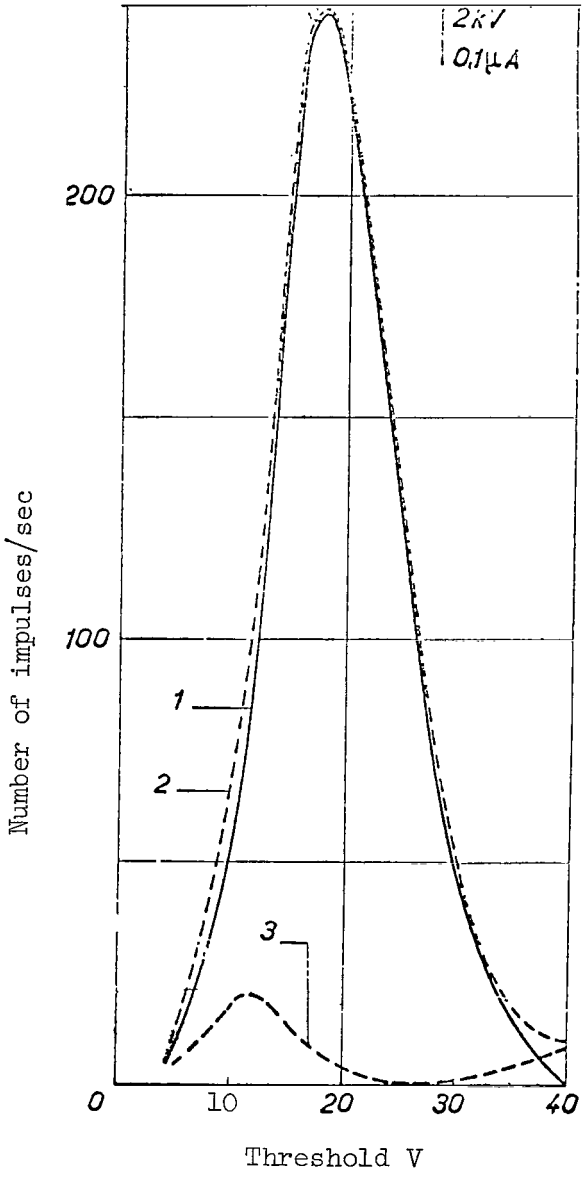

Figure 24. Nitrogen dosage in boron nitride with anticontamination device. 1, Differential curve; 2, nitrogen filter; 3, methane filter.

IX. 4. Superficial layers - contamination

Since the depth of penetration of the 2 keV electrons is very small (ref. 13), we realize at once that any superficial layer would perturb the measurements. On one hand, this layer retards the electrons and emits an X-radiation

characteristic of its components. On the other hand, this layer acts as a filter for X-rays emitted by the target below, and these X-rays are absorbed by this superficial layer.

If we examine the boron nitrate without any contamination device, we find that the nitrogen spike decreases progressively, while a very sizable spike of the carbon contained in the contamination layer appears. After 30 minutes of bombardment the nitrogen spike has completely disappeared. It is therefore impossible to perform dosages without first trapping the organic vapors present in the enclosure. Figures 23 and 24 concern boron nitrate. The first was obtained without the anticontamination device, while the second was obtained with such a device. Both measurements were made after five minutes of readings.

Let us point out that the extreme sensitivity of this method to the contamination layer could be used for the study of such layers. Even though we have not yet explored this possibility, it appears that after some reduction in the electron accelerating voltage the depth-resolving power of this method could be brought below 100 Å.

IX. 5. Filter alignment

As an example let us consider the case of nitrogen. The filters are aligned by modifying the pressure in the nitrogen and methane filters, so that the carbon line is equally transmitted on both paths (fig. 19).

When the filters are absent, and the amplitude selector is set on the carbon line, the intensity of the continuous background found on top of that line is about 1/20 of the intensity of that carbon line. A fraction of the continuous spectrum slightly in excess of 50 percent is completely absorbed after crossing the methane filter. When crossing the nitrogen filter, the continuous background is only absorbed for wavelengths λ such that $\lambda < \lambda_N = 31.1$ Å, and the transmitted intensity contains a fraction of the continuous spectrum greater than 50 percent. We therefore have a systematic error (on the order of 1/40 at most) which enters into our measurements when the filters are adjusted. A rigorous adjustment must use a characteristic line of carbon free of any continuous spectrum (fluorescence, for example).

X. Conclusion

Although we analyzed only oxygen and nitrogen, the experiments and the use of gaseous filters offer very encouraging results and suggest the extension of this method to the study of light elements. The differential filter method offers a great advantage over other methods due to the sensitivity with which the lines are detected. At the start we feared that such a method would a priori distinguish the characteristic lines very poorly, because the absorption discontinuities of the light elements are very far apart on the wavelength scale. However, the first measurements showed that the values of signal-to-noise ratio are acceptable, and for the case of oxygen and nitrogen these ratios are of the same order of magnitude as the ones obtained by dispersive methods using artificial crystals.

REFERENCES

1. Castaing, R., Doctoral Thesis, Paris, 1951. ONERA Publication No. 55, 1952.
2. Castaing, R. and Descamps, J. La Rech. Aéron., No. 63, March-April, 1958.
3. Dolby. Journal of Scientific Instruments, 40, 345, 1963.
4. Franks, A. Nature, No. 4922, 29, 1964.
5. Nicholson, J. B. and Wittry, D. B. Advances in X-Ray Analysis. Plenum Press, New York, 7, 497, 1963.
6. Henke, B. L. Advances in X-Ray Analysis. Plenum Press, New York, 7, 460, 1963.
7. Ross, P. A. Journal of the Optical Society of America, 16, 433, 1928.
8. Cambou, F. Doctoral Dissertation Faculté de Toulouse, 1955.
9. Castaing, R. and Guinier, A. Proceedings of Conference on Electron Microscopy. Delft, 1949.
10. Rossi and Stamb. Ionization Chambers and Counters. McGraw-Hill, 1949.
11. Mulvey, T. and Campbell, A. J. British Journal of Applied Physics, 9, 406, 1958.
12. Moreau, G. and Calais, D. Le journal de physique, supplément No. 6, 25, 1964.
13. Feldman, C. Physical Review, 117, No. 2, 1960.

Translated for the National Aeronautics and Space Administration
by John F. Holman Co. Inc.

"The aeronautical and space activities of the United States shall be conducted so as to contribute . . . to the expansion of human knowledge of phenomena in the atmosphere and space. The Administration shall provide for the widest practicable and appropriate dissemination of information concerning its activities and the results thereof."

—NATIONAL AERONAUTICS AND SPACE ACT OF 1958

NASA SCIENTIFIC AND TECHNICAL PUBLICATIONS

TECHNICAL REPORTS: Scientific and technical information considered important, complete, and a lasting contribution to existing knowledge.

TECHNICAL NOTES: Information less broad in scope but nevertheless of importance as a contribution to existing knowledge.

TECHNICAL MEMORANDUMS: Information receiving limited distribution because of preliminary data, security classification, or other reasons.

CONTRACTOR REPORTS: Technical information generated in connection with a NASA contract or grant and released under NASA auspices.

TECHNICAL TRANSLATIONS: Information published in a foreign language considered to merit NASA distribution in English.

TECHNICAL REPRINTS: Information derived from NASA activities and initially published in the form of journal articles.

SPECIAL PUBLICATIONS: Information derived from or of value to NASA activities but not necessarily reporting the results of individual NASA-programmed scientific efforts. Publications include conference proceedings, monographs, data compilations, handbooks, sourcebooks, and special bibliographies.

Details on the availability of these publications may be obtained from:

SCIENTIFIC AND TECHNICAL INFORMATION DIVISION

NATIONAL AERONAUTICS AND SPACE ADMINISTRATION

Washington, D.C. 20546